

# NEW DOUBLE-K CRITERION FOR CRACK PROPAGATION IN QUASI-BRITTLE FRACTURE UNDER MODERATE DYNAMIC LOADING: EXPERIMENTAL INVESTIGATION

SHILANG XU<sup>†</sup>, LIXIN DONG<sup>\*</sup> AND YAO WU<sup>†</sup>

<sup>†</sup> Institute of Advanced Engineering Structures and Materials  
College of Civil Engineering and Architecture  
Zhejiang University, 310058, Hangzhou, China  
E-mail: slxu@zju.edu.cn

<sup>\*</sup> Dalian University of Technology, 116024, Dalian, China  
Jilin Architectural and Civil Engineering Institute, 130118, Changchun, China  
E-mail: happydlx@126.com

**Key words:** Double-K Criterion, Moderate dynamic, Dynamic fracture, Crack propagation, Quasi-brittle fracture, Seismic loading range

**Abstract:** This paper presents the recent results of experimental investigations under dynamic loading aimed at disclosing the loading rate effect (mainly related to seismic loading range) on crack propagation in quasi-brittle fracture. Twenty four wedge-splitting tests were conducted using a servo-hydraulic machine under loading rates ranged from  $10^{-3}$  mm/s to  $10^1$  mm/s. Strain gauges were mounted along the ligament of the specimen to measure the crack velocity and the crack propagation. Extensometers were arranged to obtain the *P-CMOD* curves and *P-CTOD* curves. Though transient, the stage of stable process of crack propagation observed in the experiments could not be ignored compared to the entire loading procedure. And the crack tended to propagate along one dominant line at the mentioned loading rates. In order to predict the crack propagation for cracked quasi-brittle materials under dynamic loading, a new double-K criterion in which the concepts of dynamic fracture mechanics were taken into account was proposed based on experimental investigations.

## 1 INTRODUCTION

Dynamic loading on concrete structures arising from earthquakes is a topic of great practical concern. Researches during the last three decades have shown that the rate dependency of the concrete strength tends from a moderate rate dependency to excessive rate effects at high loading rates [1–6]. In comparison to other rate dependent materials, concrete exhibits its rate dependency at relatively low loading rates because of a  $10^{-3}$  m length scale of the heterogeneity [7, 8]. It has been confirmed by studies [9-23] that the time-dependence is caused by three different

effects [1, 25~31, 7] (1) the rate dependent bond-breakage process which produces the fracture surfaces, (2) the viscous behaviour of the bulk material between the cracks and (3) the inertia effect in the neighbourhood of the crack tip, which can significantly change the state of stresses and strains of the material. As far as the seismic loading rate (ranged from  $10^{-4}$  s<sup>-1</sup> to  $10^{-1}$  s<sup>-1</sup>) is concerned, the total resistance is controlled by the first two effects [25, 31-33]. During past decades, several fracture models for concrete were proposed to predict the crack propagation and to reflect the influence of the fracture process zone(FPZ) on

fracture characteristics of concrete materials, like the fictitious crack model (FCM) by Hillerborg et al. (1976)[34], the crack band model (CBM) by Bažant and Oh (1983)[35], the two parameter fracture model (TPFM) by Jenq and Shah (1985)[36], the effective crack model (ECM) by Karihaloo and Nallathambi (1990)[37] and Swartz and Refai (1987)[38], the size effect model (SEM) by Bažant, Kim and Pfeiffer (1986)[39], and the double-K model by XU and Reinhardt[40-41]. However, relative little experimental data with the fracture criterion is available for concrete under seismic loading.

In order to understand characterization of the fracture behaviour of concrete under this particular condition which is important for the design and analysis of a variety structures of civilian and military especially the large scale hydraulic structures, experiments covering the desired loading rates of five orders of magnitude (from  $10^{-3}$  mm/s to  $10^1$  mm/s) were carried out on a servo hydraulic machine. There are four commonly used methods for fracture test:(1) direct tension test, (2) three-point bend test on notched beams(TPB), (3) compact tension test(CT), and(4) wedge-splitting test(WS). In this paper, wedge-splitting test was selected as the examining method due to its distinct advantages such as no self-weight involved (counterbalanced by the supports), and enhancing the stiffness of the testing machine (by properly selecting the wedge angle)[42]. Strain-gauge technology was adopted to measure the crack-propagation velocity since it appears to be relatively stable for variety of loading rates [16, 17, 41, 42, 43] compared to high-speed photography [45-47] and acoustic emission [44]. The methodology of double-K criterion [40-42] which had been confirmed in static loading range was employed, whilst concepts of dynamic fracture mechanics were included into the former for the first time to describe the rate dependent fracture behaviour in the experiment. Emphasis was laid on the fact whether the toughening phenomenon in the post-crack stage that had been confirmed in the static condition was still nonnegligible in the seismic

loading range in the present paper. In the rest part of this paper the experimental procedure is described first. Subsequently, observations on crack velocities and *P-CMOD* curves are presented and discussed. Finally, summary and conclusions are drawn out.

## 2 EXPERIMENTAL PROCEDURE

### 2.1 Scope of test

24 wedge-splitting tests were performed under five loading rates ranged from quasi-static level to strain rate dependent level in Research and Teaching Laboratory for Civil and Hydraulic Engineering of Zhejiang University. The aim of these tests is to study the loading-rate effect on the characteristics of crack propagation in quasi-brittle fracture under loading rate related to seismic range, and then attempts were made to provide an accurate and simple enough description of crack propagation in quasi-brittle fracture based on the experimental results.

### 2.2 Geometry and fabrication of specimens

The wedge-splitting specimens were denoted in Figure 1 and the dimensions are shown in Table 1. The pre-cast notch in a specimen was made by inserting in the mold a greased 3mm-thick steel blade with a wedge-shaped angle of  $15^\circ$  at its tip. One day after casting the specimen, the steel blade was carefully loosed from the mold without damaging initial crack tip of the specimen.

All of the specimens were cast in steel molds, vibrated by a vibrating table, wrap cured for 24 hours. The cubes ( $150 \times 150 \times 150$  mm<sup>3</sup>) for the standard compressive and splitting tests were stored in water until testing at an age of 28 days. The wedge-splitting test specimens and the prisms( $250 \times 60 \times 50$  mm<sup>3</sup>) for direct tensile tests however, were first cured in water for 90 days and subsequently in the laboratory (20°C, 60% RH) until testing at  $400 \pm 20$  days after casting.

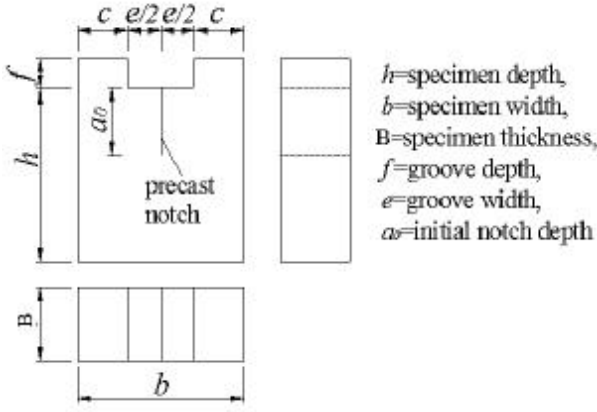


Figure 1: Geometry of a wedge splitting test specimen.

Table 1. Dimensions of a wedge splitting test specimen

$h$	$b$	$B$	$f$	$c$	$e$	$a_0$
(mm)						
200	200	200	30	75	50	80

### 2.3 Material characterization

The compositions of the adopted concrete together with the results of standard 28-day quasi-static tests are listed in Table 2. The quasi-static properties were determined by tests performed with a universal testing machine at a strain rate of  $10^{-5}$ /s. The material's characteristics of dynamic fracture mechanics are also listed in Table 2.

Table 2: Quasi-static properties of concrete tested

Mix proportions	( $\text{kg/m}^3$ )	
Portland cement	207.08	
Sand 0-2mm	722.10	
Gravel 8-10mm	298.25	
Water	81.42	
Static properties		Coefficient of variation
Density, $r$	2370 $\text{kg/m}^3$	1%
Young's modulus, $E$ (tension 400 $\pm$ 20 days)	3.062 e4	6.9%
Compressive strength, $f_c$ (28days)	34.98 MPa	6.3%
Direct tensile strength, $f_t$ (400 $\pm$ 20 days)	3.61 MPa	7.7%
Splitting strength, $f_{pt}$ (28days)	2.32 MPa	7.1%
Poisson's ratio, $u$ (assumed value)	0.2	-
Specific fracture energy $G_F$	59.629 N/m	8%
Longitudinal wave speed $v_L = \sqrt{\frac{E(1-n)}{r(1+n)(1-2n)}}$	3788.85 m/s	-
Shear wave speed $v_s = \sqrt{\frac{E}{2r(1+n)}}$	2320.19 m/s	-
Rayleigh wave speed $v_R = \frac{v_s(0.862+1.14n)}{(1+n)}$	2107.50 m/s	-
characteristic length $l_{ch}$	141.1 mm	-
characteristic time $t_{ch}$	37.2 $\mu\text{s}$	-

### 2.4 Testing equipment

The wedge-splitting tests under position control were performed on a closed-loop electro-hydraulic loading machine of 1000 KN

capacity in tension and compression with precision of 0.1 % ( see Figure 2). For the sake of comparison, four specimens were tested at the quasi-static level ( $1.2 \times 10^{-3}$  mm/s). Four rate dependent loading rates ( $1.2 \times 10^{-2}$  mm/s, 0.12mm/s, 1.2mm/s and 12mm/s) were applied.

Five specimens were tested at each of these four loading rates. Two extensometers with an accuracy of 0.1% were used. One was amounted to measure the crack mouth opening displacement ( *CMOD* ). The other was arranged for the opening displacement at the crack tip ( *CTOD* ). In order to observe the time at which the crack tip of the FPZ transited, 12 strain gauges (M1-M6 and B1-B6, 20mm in length and 5 mm in width) were bonded to the polished specimen surface. Since a running crack in concrete is often deflected by aggregates along its path, 6 gauges were bonded in the middle column along the axis of the initial crack line with a distance of 20 mm between each neighboring gauge, and the other 6 gauges were bonded along the axis 20 mm away from the initial crack line in the same way. All test data were collected through auto data acquisition system synchronously with the sample rate set at 10 kHz.

### 3 THE EXPERIMENTS AND RESULTS

#### 3.1 Fracture configuration

According to theoretical and experimental investigations available, as well as numerical studies, failure mode, crack pattern and velocity of the crack propagation are influenced by the loading rate [25,32-34,50,51]. Principally, with increase of loading rate failure mode tends to change from mode-I to mixed mode [52]. It's the inertia force that plays the most significant role in these changes, since it homogenizes material in the fracture process zone and reduces crack to move away from the zone of high inertia forces. In the case of the loading rates that the present paper refers to (within low and moderate loading range), mode-I failure could be reasonable. And the fracture configuration observed in the experiment confirmed the above point of view. And in every wedge splitting test carried out at each of the five loading rates, the crack tended to propagate along one dominant line, see Figure 3 for the typical trace of the crack propagation.

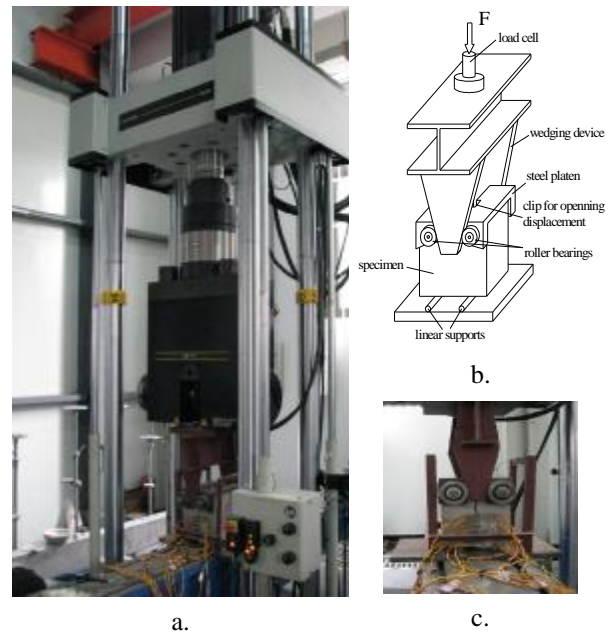


**Figure 2:** Wedge splitting test setup: (a) View of the testing equipment, (b) transmission device and supports for the wedge splitting test, (c) an arranged specimen with gauges.

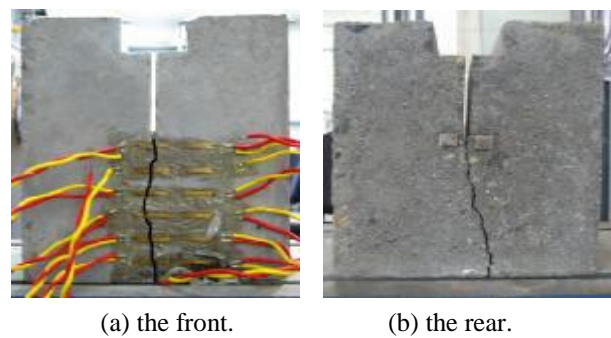


**Figure 3:** Typical crack trace of the specimens

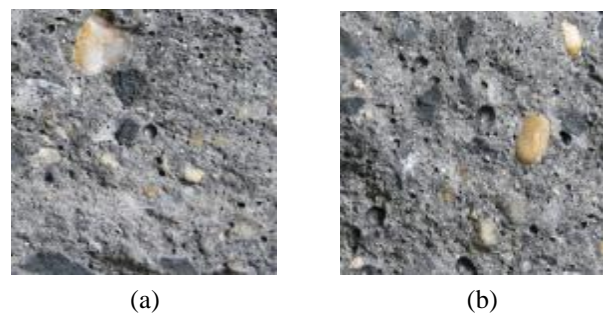


**Figure 4:** Typical fracture sections:  
 (a) rate dependent level: 0.012 mm/s ~ 12mm/s  
 (b) quasi-static level: 0.0012 mm/s

By contrast the fracture sections obtained at the rate dependent levels with the ones obtained at quasi-static level shown in Figure

4, it is obvious that when the loading rate ranged from 0.012 mm/s to 12mm/s (ranged from the magnitude of  $10^{-4}$ /s to  $10^{-1}$ /s) almost all of the large aggregates in the fracture section were split, while for the loading rate of 0.0012 mm/s (at the magnitude of  $10^{-5}$ /s), a portion of the large aggregates were split and most aggregates were bypassed, namely, the failure tended to take place at the interface. Such difference would lead to higher energy consumption for the rate dependent ones than the quasi-static ones, what is later confirmed by the *P-CMOD* curves.

### 3.2 Crack velocity and crack initiation

The crack velocity refers to the speed in which the initiated cohesive crack tip will propagate. When the crack initiates, an unloading stress wave is generated. So the strain-gauge technology which is relatively straight forward was employed to capture the sudden decrease of stress. The strain gauges arranged along the initial crack line were named as M1 to M6 respectively, and the ones along the axis 20mm from the initial crack line were named as B1 to B6 respectively. When the crack propagates along or bypasses a certain gauge the strain tends to change abruptly. The transformation of the stress with time could be reflected clearly by the strain history of M1 to M6. The time interval that the stress wave transferred from the crack line to gauge B1 to B6 could be ignored in that the stress wave speed is much greater than the velocity of crack propagation[48]. Thus the time of peak strain of each gauge from B1 to B6 could well reflect the time when the crack propagated at each loading rate. The average crack-velocity was obtained through dividing the distance between two neighboring strain gauges (20mm) by the time interval across the two corresponding peak signals. The time when the crack initiated was determined by the point B1 reached its peak value; meanwhile the *P-ε* curves of M1 began to show its

remarkable nonlinearity which was later given in Figure 5.

Combining the strain histories of the different six strain gauges in one row, the average strain rates and crack velocities were obtained in Table 3. When calculating the average pre-peak strain rates ( $\dot{\epsilon}$ ) of B2 to B6 at each loading rate, the amount of time of one strain gauge was added up by the summation of all the time intervals above it.

It is shown in Table 3 that for the strain gauges of the same position the crack velocities tend to have an obvious increase along with the loading rate, even five orders of magnitude when the loading rate ( $\dot{\epsilon}$ ) varies from  $10^{-5}\text{s}^{-1}$  to  $10^{-1}\text{s}^{-1}$ . This remarkable variation indicates that for the low or moderate dynamic loading range, especially for the seismic loading rates, the rate dependence is significant and the crack velocity should be involved in the description of fracture process.

For the static or quasi-static loading rate, excessive experimental investigations have shown that the fracture process in concrete structures includes three different stages: crack initiation, stable crack propagation and unstable fracture (or failure). This is also observed in the experiment of rate-dependent loading in this paper. In Table 3, it is obvious that the ratio of post-crack time to total loading time are very close for all the loading rate mentioned, which indicates that from the sense of time, similar to the quasi-static condition, the post-crack stage should not be ignored compared to the entire loading procedure for the rate dependent loading rates. Also, the crack velocities in Table 3 provide more visual support of the two stages after crack initiation: for the same loading rate, the crack velocities from B1 to B4 keep relatively stable, whereas the crack velocities of B5 and B6 show abrupt increase. That is to say after crack initiation which takes place when B1 reaches its peak strain, there is a stage of stable crack propagation from B1 to B4. And then from B5 to B6, the unstable propagation of the crack begins which indicates the failure.

**Table 3:** Crack velocity and strain rate in the experiment.

Loading rate $\dot{d}$ (mm/s)	Total loading time(s)	Ratio of post-crack time to total time	Gauge number	Time of peak strain (s)	Time interval (s)	crack velocity (m/s)	Pre-peak $\dot{\epsilon}$ ( $s^{-1}$ )
12	0.624	0.119	B1	28.84800	0.5496	-	0.128146
			B2	28.86509	0.01709	1.170275	0.366103
			B3	28.90095	0.03586	0.557724	-0.17311
			B4	28.91011	0.00916	2.183406	0.170952
			B5	28.91502	0.00491	4.07332	0.162119
			B6	28.91699	0.001965	10.17812	0.087443
1.2	4.5977	0.086	B1	5.645460	4.20236	-	12.29E-3
			B2	5.73200	0.08654	0.231107	35.06 E-3
			B3	5.82750	0.0955	0.209424	-17.67 E-3
			B4	6.02150	0.194	0.103093	19.49 E-3
			B5	6.04029	0.01879	1.064396	21.45 E-3
			B6	6.04271	0.00242	8.264463	10.84 E-3
0.12	62.034	0.059	B1	145.75996	58.37696	-	0.001026
			B2	148.41460	0.17766	0.112575	0.002955
			B3	149.28400	0.8694	0.023004	-0.00146
			B4	149.46166	0.17766	0.112575	0.001595
			B5	149.46395	0.00229	8.733624	0.000677
			B6	149.46604	0.00209	9.569378	0.000347
0.012	455.82 6	0.098	B1	552.1390	410.762	-	0.000126
			B2	577.68441	25.5454	0.000783	0.000276
			B3	596.84343	19.159	0.001044	-0.00032
			B4	597.36226	0.51886	0.038546	0.000226
			B5	597.67063	0.30837	0.064857	0.000288
			B6	597.67401	0.003381	5.91541	0.000133
0.0012 (quasi-static)	12527	0.067	B1	26.47831	12500	-	6.75E-06
			B2	26.95172	0.4734	4.23E-05	2.59E-05
			B3	27.17816	0.22646	8.83E-05	-8.56E-06
			B4	27.25212	0.07394	0.000270	5.62E-06
			B5	27.27195	0.01985	0.001008	1.16E-05
			B6	27.27402	0.002071	0.009657	1.88E-06

### 3.3 $P-\epsilon$ curves and $P-CMOD$ curves

$P-\epsilon$  curve is commonly utilized in research of concrete since it well represents the variation

of strain field along with the load. In the investigation by John and Shah it was found that the starting point of the nonlinear segment of the load-time curve corresponded to such a

point of strain-time curve at which the strain began to rise rapidly [53]. Similar feature is detected in the rate-dependent experiment mentioned in this paper without exception. The typical curves of the loads versus the strains of M1 at each rate-dependent loading rate are given in Figure 5. The  $P_{ini}$  defined as the load at which the crack initiated is determined by the points when the strain-time curves of M1 and B1 started to vary abruptly. It is obvious in the  $P-e$  curves for the strain rates of  $10^{-4}s^{-1}$  to  $10^{-1}s^{-1}$  that before the point of  $P_{ini}$  the curves behave linear basically, whereas after this key point remarkable nonlinearity is present. It is

also shown in the  $P-e$  curves that when the  $P_{ini}$  is exceeded the bearing capacity of the specimen has a relatively large increase which is mostly caused by the viscous behavior of the bulk material between the cracks.

Typical  $P$ -CMOD curves at each loading rate are presented in Figure 6 with experimental results of  $P_{ini}$  and  $P_{max}$  followed in Table 4, where the key point defined as  $P_{ini}$  occurs at the starting point of the nonlinear segment of  $P$ -CMOD curve, and the largest peak value defined as  $P_{max}$  occurs corresponding to the maximum loading point at  $P$ -CMOD curve.

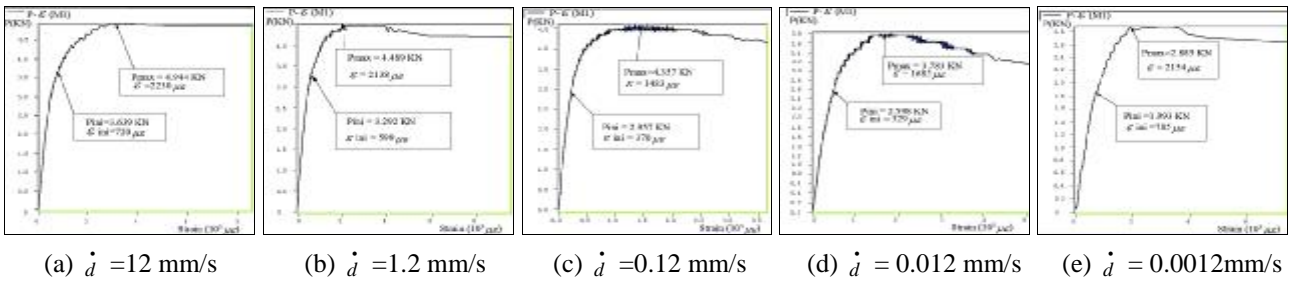


Figure 5: Typical  $P-e$  curves at each loading rate ( $\dot{d}$ )

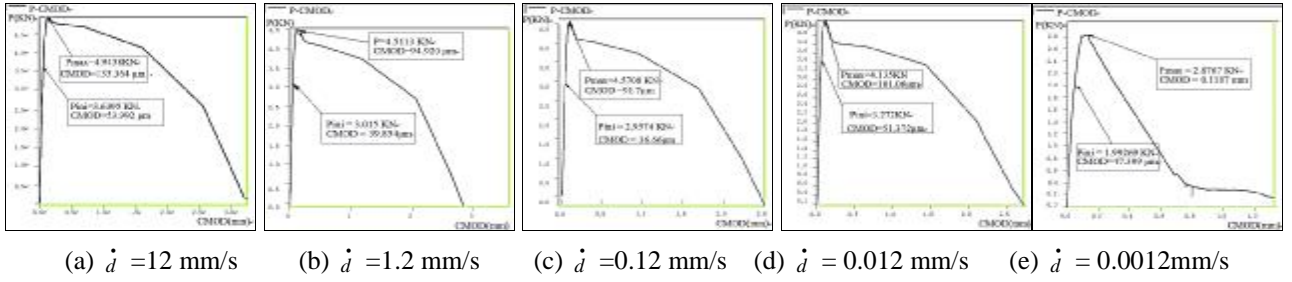


Figure 6: Typical  $P$ -CMOD curves at each loading rate ( $\dot{d}$ )

Table 4. Experimental results of  $P_{ini}$  and  $P_{max}$

Loading rate $\dot{d}$ (mm/s)	$P_{ini}$ detected by $P-e$ curve (KN)	$P_{ini}$ detected by $P$ -CMOD curve (KN)	$P_{max}$ (KN)
12	3.639(7%*)	3.485(6%*)	4.967(8%*)
1.2	3.446(8%*)	3.182(5%*)	4.498(3%*)
0.12	3.183(5%*)	2.957(3%*)	4.359(6%*)
0.012	2.985(8%*)	2.728(7%*)	3.942(8%*)
0.0012 (quasi-static)	2.235(6%*)	2.056(5%*)	3.013(5%*)

\*denotes the coefficient of variation

The complete curves indicate that the area under the  $P$ -CMOD curves which represent the energy consumed by the fracture process tended to increase with the loading rate. This coincides with the phenomenon disclosed in the fracture configuration shown in Figure 4. Partial enlarged details of  $P$ -CMOD curves show significant difference between linear segment and nonlinear segment which are distinguished by  $P_{ini}$ . The collected results of  $P_{ini}$  and  $P_{max}$  are given in Table 4. It is noteworthy that, at each rate-dependent loading rate mentioned in the experiment, the nonlinear segment after  $P_{ini}$  cannot be omitted since it is almost larger than 25% of the  $P_{max}$  in magnitude. It means that for moderate dynamic loading range, there is

also a segment of stable crack propagation after the crack initiation in which the bearing capacity keeps on growing considerably. In other words, the material tends to toughened after  $P_{ini}$ . It demonstrates again the argument proposed by van Mier [54] that Crack bridges are formed at the final failure stage which has also been confirmed by in J. Weerheijm's the dynamic research [55].

The curves also show that both  $P_{ini}$  and  $P_{max}$  presented ascending tendency along with the loading rate. Moreover, the contribution of the nonlinear segment is somehow larger in the rate-dependent loading range than in the quasi-static condition. The reason is the increase tendency of the tensile strength with the loading rate [56] which usually acts as the decisive factor in the fracture process for quasi-brittle materials. This consequent increase of  $P_{ini}$  and  $P_{max}$  indicates that rate-dependency should be taken into account when describing

#### 4 NEW DOUBLE-K CRITERION UNDER MODERATE DYNAMIC LOADING

Incorporation with the aforementioned experimental results, it is evident that for strain rate ranged from  $10^{-4}s^{-1}$  to  $10^{-1}s^{-1}$ , the fracture of concrete behaves the quasi-brittle characteristic. That is, for this strain rate range the fracture process of concrete covers three distinct stages: (1) the stage of primary elastic when the crack remains the original notch, (2) the stage of stable crack propagation beginning with the crack initiation, in which the bearing capacity keeps on growing considerably, (3) the stage of unstable crack propagation after the maximum load is reached in which the crack propagates at a velocity extremely larger than in the second stage, namely, the so called failure stage. This experimentally observed quasi-brittle fracture behavior is similar to the static or quasi-static condition. Thus, the methodology of double-K criterion [40-42] which has already been verified to well represent the fracture response of quasi-brittle materials like concrete for the static or quasi-static condition is adopted. Likewise, the fracture process is described with the stress

the fracture behavior under low or moderate dynamic loading, especially the seismic loading.

By contrast the  $P$ -CMOD curve with the  $P$ - $e$  curve at each loading rate respectively, it can be seen that the  $P_{ini}$  detected were very close, however the  $P_{ini}$  in the former ones are somehow a bit smaller than the later, shown in Table 4. That is, the  $P$ -CMOD curve is a little more sensitive to the stable crack propagation than  $P$ - $e$  curve. This is because that both the stable crack propagation and the unstable fracture belong to a localized behavior of strain concentration in a structure and the crack mouth opening displacement is a local variable which is mainly affected by the crack opening. Thus the  $P$ -CMOD curve maybe a better choice when the crack initiation load  $P_{ini}$  is to determined, while the  $P$ - $e$  curve maybe utilized as a relatively broad check.

intensity factors, whereas concepts of dynamic fracture mechanics are employed and rate-dependency is taken into account according to the experiment results. The stress intensity factors are denoted as  $K$  and  $K_d$  with the sub "d" to differentiate from the static condition for later discussion.

In the first stage, both the material characteristic and the geometry configuration act as the original condition. Linear-elastic dynamic fracture mechanics principles are available. Thus the stress intensity factor history should take the form as follows:

$$K(t) = K(P(t), a_0, B, h) \quad (1)$$

Where,

$P(t)$  denotes the applied load at an arbitrary time before crack initiation;

$a_0$  denotes the initial depth of the notch;

$B$  denotes the thickness of the specimen;

$h$  denotes the depth of the specimen.

In the second stage, the length of the crack keeps on growing because of the crack propagation. And the nonlinear toughening phenomenon of the material in the field near the crack tip is onset along with the rate-

dependent characteristic. The toughening stress intensity factor caused by the so called cohesive stress history between the crack surfaces could be expressed as such:

$$K_{ld}^{coh}(t) = k(v)K_{ld}(a_e(t), \dot{e}) \quad (2)$$

Where  $K_{ld}(a_e(t), \dot{e})$  is the time related cohesive stress intensity factor in which  $a_e(t)$  denotes the effective crack length [41, 57, and 58]. The factor  $k(v)$  is a dimensional function of the material crack velocity  $v$ , and it is also related to the Rayleigh wave speed  $v_R$  and the longitudinal wave speed  $v_L$  of the material.

Thus the stress intensity factor history in this stage should take the form as follows:

$$K(t) = K_{ld}^{coh}(t) + K_{ld}^{ini} \quad (3)$$

Finally, the unstable stress intensity factor according to the dynamic fracture mechanics for a moving crack, takes the form as follows:

$$K_{ld}^{un} = 2k(\dot{a}_{un}(t)) \frac{\sqrt{(1-2u)/p}}{(1-u)} \int_0^{t_{un}} \sqrt{v_L(t_{un}-t)} \frac{dp(t)}{dt} dt \quad (4)$$

Where  $u$  denotes the Poisson's ratio;  $k(a(t))$  is the universal function of crack tip speed as in equation (2), with  $\dot{a}(t)$  denoting the derivative of the effective crack length  $a_e(t)$ ;  $t_0$ ,  $t_{un}$  denotes the original loading time and the unstable time respectively;  $dp(t)$  represents the infinitesimal magnitude of the applied load.

The new double-K criterion for the moderate dynamic loading could be described briefly as follows:

When

$K(t) < K_{ld}^{ini}$ , the crack remains as original;

$K(t) = K_{ld}^{ini}$ , the crack growth begins;

$K_{ld}^{ini} < K(t) < K_{ld}^{un}$ , the propagating crack develops steadily;

$K(t) = K_{ld}^{un}$ , the unstable crack propagation is onset;

$K(t) > K_{ld}^{un}$ , the crack propagates unsteadily.

For a notched structure with an arbitrary geometrical configuration in practice, the stress intensity factor  $K(t)$  at the crack tip can be evaluated by an analytical solution, or a numerical approach using a finite element code. Thus for the structure of a given material, this new double-K fracture criterion for rate-dependent loading (strain rate ranged from  $10^{-4}s^{-1}$  to  $10^{-1}s^{-1}$ ) is available to determine the important issues like: whether the crack will grow or whether it will propagate steadily, which are of great significant for the safety judgment of special structures like dams and vessels of a nuclear reactor, especially under seismic loading.

## 5 SUMMARY AND CONCLUSIONS

In the present paper the rate-dependent fracture behavior of concrete concerning the seismic loading is studied through wedge-splitting tests. The tests were performed on a closed-loop electro-hydraulic loading machine covering a wide range of loading rates, from  $10^{-3}$  mm/s to  $10^1$  mm/s. And strain-gauges and extensometers were employed to measure the strain and displacement of the crack opening. The methodology of double-K criterion is adopted incorporation with the concepts of dynamic fracture mechanics according to the experimental results. The following conclusions can be drawn.

- (1) For the strain rate ranged from  $10^{-4}s^{-1}$  to  $10^{-1}s^{-1}$  the crack propagates along one dominant line. And higher energy consumption is needed for the higher loading rate;
- (2) the crack velocities have an obvious rate effect along with the loading rate and should be involved in the description of fracture process;
- (3) the fracture process for this loading range includes three different stages: elastic stage before the crack initiation, stable crack propagation and unstable fracture;
- (4) the material toughening phenomenon due

to the dynamic cohesive forces is remarkable; (5) the increase tendency of the tensile strength with the loading rate has a significant influence in the rate-dependent fracture; (6) the  $P$ -CMOD curve is a little more sensitive to the crack initiation load  $P_{ini}$  than the  $P$ - $e$  curve, while the strain gauge technology is a good method of gaining the crack velocity. Finally, the new double-K criterion under the mentioned loading rate is proposed which is promising in the safety judgment of structures like dams and vessels of a nuclear reactor.

## REFERENCES

- [1] Reinhardt H.W. Concrete under impact loading, tensile strength and bond. *Heron* 1982; 27(3).
- [2] Ross C.A., Kuennen S.T., Strickland W.S. High strain rate effects on tensile strength of concrete. In: Proceedings on the interaction of non-nuclear munition with structures, Panama City Beach, FL, April 1989. p. 302–8.
- [3] Lambert D.E., Ross CA. Strain rate effects on dynamic fracture and strength. *Int J Impact Eng* 2000;24(10):985–98.
- [4] Chandra D., Krauthammer T. Rate sensitive micromechanical model for concrete. In: Bounds W, editor. Concrete and blast effects, ACI SP-175, 1998. p. 281–305.
- [5] Shah S.P., John R. Strain rate effects on Mode I crack propagation in concrete. In: Wittmann F.H., editor. Fracture toughness and fracture energy of concrete. *Developments in Civil Engineering*, vol. 18. Amsterdam: Elsevier; 1986.
- [6] Klepaczko J.R., Brara A. An experimental method for dynamic tensile testing of concrete spalling. *Int J Impact Eng* 2001;25(4):387–409.
- [7] Weerheijm J. Concrete under impact tensile loading and lateral compression. Doctoral thesis, Delft University, 1992.
- [8] Weerheijm J. Properties of concrete under dynamic loading 3. Fracture model for brittle materials. PML report, PML 1990-65, Rijswijk, October 1990.
- [9] Shah S.P., Chandra S. “Fracture of concrete subjected to cyclic and sustained loading.”. *ACI Journal* 1970;67(10):816–25.
- [10] Zielinski A.J. Model for tensile fracture of concrete at high-rates of loading. *Cement and Concrete Research* 1984;14(2):215–24.
- [11] Biolzi L., Tognon G. Strain rate effect on crack-propagation in concrete. *Theoretical and Applied Fracture Mechanics* Jun 1987;7(3):201–6.
- [12] Wittmann P.E., Roelfstra PE, Mihashi H, Huang Y-Y, Zhang X-H, Nomura N. Influence of age of loading, water-cement ratio and rate of loading on fracture energy of concrete. *Materials and Structures* 1987;20:103–10.
- [13] Oh B.H. Fracture-behaviour of concrete under high-rates of loading. *Engineering Fracture Mechanics* 1990;35(1–3):327–32.
- [14] Reinhardt H.W., Weerheijm J. Tensile fracture of concrete at high loading rates taking into account inertia and crack velocity effects. *International Journal of Fracture* Sep 1 1991;51(1):31–42.
- [15] Bažant Z., Gettu R. Rate effects and load relaxation in static fracture of concrete. *ACI Materials Journal* Sep–Oct 1992;89(5):456–68.
- [16] Yon J-H, Hawkins N.M., Kobayashi A.S. Strain-rate sensitivity of concrete mechanical-properties. *ACI Materials Journal*. Mar–Apr 1992;89(2):146–53.
- [17] Du J., Yon J-H, Hawkins NM, Arakawa K, Kobayashi AS. “Fracture process zone for concrete for dynamic loading.”. *ACI Materials Journal* May–Jun 1992; 89(3):252–8.
- [18] Bažant Z., Gu WH, Faber KT. Softening reversal and other effects of a change in loading rate on fracture of concrete. *ACI Materials Journal* Jan–Feb 1995;92(1):3–9.
- [19] Bažant Z., Li YN. Cohesive crack with rate-dependent opening and viscoelasticity: I. mathematical model and scaling. *International Journal of Fracture* 1997;86(3):247–65.
- [20] Rossi P., Van Mier JGM, Toutlemonde F, Le Maou F., Boulay C. Effect of loading rate on the strength of concrete subjected to uniaxial tension. *Materials and Structures* Jun 1994; 27(169):260–4.
- [21] Rossi P., Toutlemonde F. Effect of loading rate on the tensile behaviour of concrete: description of the physical mechanisms. *Materials and Structures* Mar 1996; 29(186):116–8.

- [22] Weerheijm J., Van Doormaal A. Tensile failure of concrete at high loading rates: new test data on strength and fracture energy from instrumented spalling tests. *International Journal of Impact Engineering* Mar 2007;34(3):609–26.
- [23] Ruiz G., Pandolfi A., Ortiz M. Three-dimensional cohesive modeling of dynamic mixed-mode fracture. *International Journal for Numerical Methods in Engineering* 2001; 52:97–120.
- [24] Bischoff, P., Perry, S., 1991. Compressive behaviour of concrete at high strain rates. *Materials and Structures/ Matériaux et Constructions* 24, 425–450.
- [25] Ozbolt, J., Reinhardt, H.W., 2005. Rate dependent fracture of notched plain concrete beams. In: Pijaudier-Cabot, Gerard, Acker (eds.). *Proceedings of the Seventh International Conference CONCREEP-7*, pp. 57–62.
- [26] Pedersen, R. R., Simone, A., Sluys, L. J., 2006. Continuous-discontinuous modelling of dynamic failure of concrete using a viscoelastic viscoplastic damage model. In: Mota Soares, C.A. et al. (eds.). *III European Conference on Computational Mechanics*, Lisbon, Portugal.
- [27] Pedersen, R. R., 2009. *Computational Modelling of Dynamic Failure of Cementitious Materials*, Dissertation. TU Delft, The Netherlands.
- [28] Larcher M., Development of discrete cracks in concrete loaded by shock waves. *International Journal for Impact Engineering* 2009, 36, 700–710.
- [29] fib, 2010. *New Model Code*, Chapter 5, Code-type models for concrete behavior (Draft).
- [30] Wu Z.S., Bažant Z. Finite element modeling of rate effect in concrete fracture with influence of creep. In: Bažant, Carol, editors. “Creep and shrinkage of concrete”, *Proceedings of the fifth international RILEM symposium*. London: E & FN Spon; 1993. p. 426–32 [ISBN 0419 18630 1].
- [31] Ozbolt, J., Rah, K.K., Mestrovic, D., 2006. Influence of loading rate on concrete cone failure. *International Journal of Fracture* 139, 239–252.
- [32] Travaš, V., 2009. *Three-dimensional Finite Element Formulation for Concrete Failure at High Energy Impact Loadings*. Dissertation, Faculty of Civil Engineering Rijeka, Croatia.
- [33] Travaš, V., Ozbolt, J., Kozar, I., 2009. Failure of plain concrete beam at impact load: 3D finite element analysis. *International Journal of Fracture* 160, 31–41.
- [34] Hillerborg, A., Modeer, M. and Petersson, P.E. (1976). Analysis of crack formation and crack growth in concrete by means of fracture mechanics and finite elements. *Cement and Concrete Research* 6, 773–782.
- [35] Bažant, Z.P. and Oh, B.H. (1983). Crack band theory for fracture of concrete. *RILEM, Materials and Structures* 16(93), 155–177.
- [36] Jenq, Y.S. and Shah S.P. (1985). Two parameter fracture model for concrete. *Journal of Engineering Mechanics, ASCE*, 111(10), 1227–1241.
- [37] Karihaloo, B.L. and Nallathambi, P. (1990). Effective crack model for the determination of fracture toughness  $K_{Ic}$  of concrete. *Engineering Fracture Mechanics* 35(4/5), 637–645.
- [38] Refai, T.M.E. and Swartz, S.E. (1987). *Fracture Behavior of Concrete Beams in Three-Point Bending Considering the Influence of Size Effects*. Report No. 190, Engineering Experiments Station, Kansas State University.
- [39] Bažant, Z.P., Kim, J.K. and Pfeiffer, P.A. (1986). Determination of fracture properties from size effect tests. *Journal of Structural Engineering, ASCE*, 112 (2), 289–307.
- [40] Xu Shilang and Reinhardt H.W., Determination of double-K criterion for crack propagation in quasibrittle materials: Part I – Experimental investigation of crack propagation, *International Journal of Fracture*, 98: 111–149, 1999.
- [41] Shilang Xu and Reinhardt H.W. Determination of double-K criterion for crack propagation in quasi-brittle fracture, Part II: Analytical evaluating and practical measuring methods for three-point bending notched

- beams, *International Journal of Fracture* 98: 151–177
- [42] Shilang Xu and Reinhardt. H. W. Determination of Double-K Criterion for Crack Propagation in Quasi-Brittle Materials part III: Compact Tension Specimens and Wedge Splitting Specimens. *International Journal of Fracture*, Vol. 98, Issue 2, 1999, (179-193).
- [43] May IM, Chen Yi, Owen DRJ, Feng Y, Thiele PJ. Reinforced concrete beams under drop-weight impact loads. *Computers and Concrete* Apr–Jun 2006; 3(2–3):79–90.
- [44] Beppu M., Miwa K., Itoh M., Katayama M., Ohno T. Damage evaluation of concrete plates by high-velocity impact. *International Journal of Impact Engineering* Dec 2008;35(12):1419–26.
- [45] Maji A.K., Ouyang C., Shah S.P. Fracture mechanics of quasi-brittle materials based on acoustic emission. *Materials Research Society* 1990;5(1):206–17.
- [46] Zehnder A.T., Rosakis A.J. Dynamic fracture initiation and propagation in 4340 steel under impact loading. *International Journal of Fracture* 1990;43: 271–85.
- [47] Mindess S., Bentur A. “A preliminary study of the fracture of concrete beams under impact loading, using high-speed photography,”. *Cement and Concrete Research* 1985;15(3):474–84.
- [48] Mindess S. Crack velocities in concrete subjected to impact loading. *Canadian Journal of Physics* May–Jun 1995;73(5-6):310–4.
- [49] Freund L.B. *Dynamic fracture mechanics*. Cambridge: The Press Syndicate of the University of Cambridge; 1998.
- [50] Freund, L.B., 1972a. Crack propagation in an elastic solid subjected to general loading-I. Constant rate of extension. *Journal of the Mechanics and Physics of Solids* 20, 129–140.
- [51] Freund, L.B., 1972b. Crack propagation in an elastic solid subjected to general loading-II. Non-uniform rate of extension. *Journal of the Mechanics and Physics of Solids* 20, 141–152.
- [52] Joško Ožbolt, Akanshu Sharma, Hans-Wolf Reinhardt. Dynamic fracture of concrete – compact tension specimen *International Journal of Solids and Structures* 48 (2011) 1534–1543.
- [53] John, R. and Shah, S.P. (1986). Fracture of concrete subjected to impact loading. *Journal of Cement and Concrete Aggregation* 8(1), 24–32.
- [54] van Mier JGM. *Fracture processes of concrete*. Boca Raton: CRC Press, Inc.; 1997.
- [55] J. Weerheijm, J.C.A.M. Van Doormaal. Tensile failure of concrete at high loading rates: New test data on strength and fracture energy from instrumented spalling tests *International Journal of Impact Engineering* 34 (2007) 609–626.
- [56] CEB Comite Euro-International du Beton. *Concrete structures under impact and impulsive loading*. Bulletin d’ Information No. 187, August 1988.
- [57] Jenq, Y.S. and Shah, S.P. (1985a). A fracture toughness criterion for concrete. *Engineering Fracture Mechanical* 21(5), 1055–1069.
- [58] Jenq, Y.S. and Shah, S.P. (1985b). Two parameter fracture model for concrete. *Journal Engineering Mechanical, ASCE* 111(10), 1227–1241.